Vol 18 No 11, November 2009
1674-1056/2009/18(11)/4823-06

Chinese Physics B

© 2009 Chin. Phys. Soc.
and IOP Publishing Ltd

Dynamic splitting and merging of an atom cloud on an atom chip*

Ke Min(柯 敏), Yan Bo(颜 波),
Cheng Feng(程 峰), and Wang Yu-Zhu(王育竹)†

The Laboratory of Quantum Optics, Shanghai Institute of Optics and Fine Mechanics, Chinese Academy of Sciences, Shanghai 201800, *China*

Center for Cold Atom Physics, Chinese Academy of Sciences, Shanghai 201800, *China*

(Received 9 December 2008; revised manuscript received 23 February 2009)

Chip-based atom interferometers bring together the advantages of atom chips and Bose–Einstein condensates. Their central prerequisite is that a condensate can be coherently split into two halves with a determined relative phase. This paper demonstrates the dynamical splitting and merging of an atom cloud with two U-wires on an atom chip. Symmetrical and asymmetrical splittings are realized by applying a bias field with different directions and magnitudes. The trajectories of the splitting are consistent with theoretical calculations. The atom chip is a good candidate for constructing an atom interferometer.

Keywords: atom chip, dynamic splitting and merging, chip-based atom interferometers

PACC: 3280P

Recently there has been rapid progress in the precise control and manipulation of cold neutral atoms on an atom chip.[1] In particular, the realization of Bose–Einstein condensation on atom chips[2,3] make coherent manipulation of matter waves on a microscale feasible. An atom chip combined with Bose–Einstein condensed atoms which have uniform quantum phase has opened the way for chip-based atom interferometers with Bose–Einstein condensates. Compared with traditional atom interferometers,[4] chip-based atom interferometers have some advantages of small size, robust geometries, large enclosed area and so on. Therefore, they will be very useful as inertial sensors in the future.[5] Up to now, a variety of pioneering experiments has already been done toward this goal, such as coherent splitting in momentum space[6−8] and dynamically deforming a single potential well into two potential wells.[9−15]

In this paper, we study the dynamical splitting and merging of an atom cloud in a magnetic double well potential generated by two U-wires on an atom chip. Applying a bias field perpendicular to the central parts of U-wires, we succeeded in realizing horizontally symmetrical splitting and merging of an atom cloud. Changing the direction and magnitude of the bias field, we observe asymmetrical splitting. Moreover we investigate the trajectories of symmetrical and asymmetrical splitting, which are consistent with theoretical calculations.

A magnetic double well potential was realized with an atom chip using a two U-wire scheme,[16] which is a modified version of the two-wire scheme proposed in Ref.[9]. The schematic diagram is shown in Fig.1(a). As known, in the two-wire scheme, when current I in the x direction is sent through two chip wires, and a bias field B_y less than a critical field magnitude $B_{\rm c} = \mu_0 I/\pi d$, is applied in the y direction, two lines of local minima in the magnetic field which have a quadruple field configuration will be generated on the perpendicular bisector of two wires, where μ_0 is the permeability of the vacuum and d is the distance between the two wires. As the magnitude of the bias field B_y is increased, the two minima move toward each other and coalesce to form a single guide located at $d/2$ away from the chip surface at the critical bias field $B_{\rm c}$. At a higher B_y, the single guide splits symmetrically into a double well in the horizontal direction again. In our double U-wire, something is different. First, considering the finite length of the central parts of the U-wires, which is 800 μm, the critical bias field $B_{\rm c}$ is less than $\mu_0 I/\pi d$, and the double wells do not merge at $d/2$ away from the chip surface.

*Project supported by the State Key Basic Research Program of China (Grant No 2006CB921202) and the National Natural Science Foundation of China (Grant No 10334050).

†Corresponding author. E-mail: yzwang@mail.shcnc.ac.cn

In our case, $I = 3$ A, d=880 μm, the critical field B_c is about 7.7×10^{-4} T, and the merge point is about 340 μm away from the chip surface. Second, when B_y is less than 7.7×10^{-4} T, the two quadruple guides merge together near the end of the central parts of U-wires and form an asymmetrical 'ring', as shown in Fig.1(b). It must be mentioned that the bent leads of the two U-wires contribute nothing to the confinement along the x direction, because they are symmetrically arranged on opposite sides of the yz plane. The confinement along x is produced by the central parts with finite length.[17] The lower half of the 'ring' which is close to the chip has a higher gradient, consequently the loading efficiency is probably quite small. If the parameters of two U-wires are properly chosen, it is possible to realize a nearly symmetrical 'ring'. Like the two-wire scheme, when the bias field B_y increases to 7.7×10^{-4} T, the ring-like trap coalesces to form a single hexapole trap where the gradient vanishes. If the bias field B_y is increased further, the hexapole trap again splits symmetrically into two three-dimensional quadruple traps in the horizontal direction. Here, the minima of two quadruple traps are not at the xz plane, thus the symmetry of the bent leads is broken down, and then the confinement along the x direction is offered by the bent leads of the U-wires. The distance between two traps increases with the bias field, as well as the gradients of two traps.

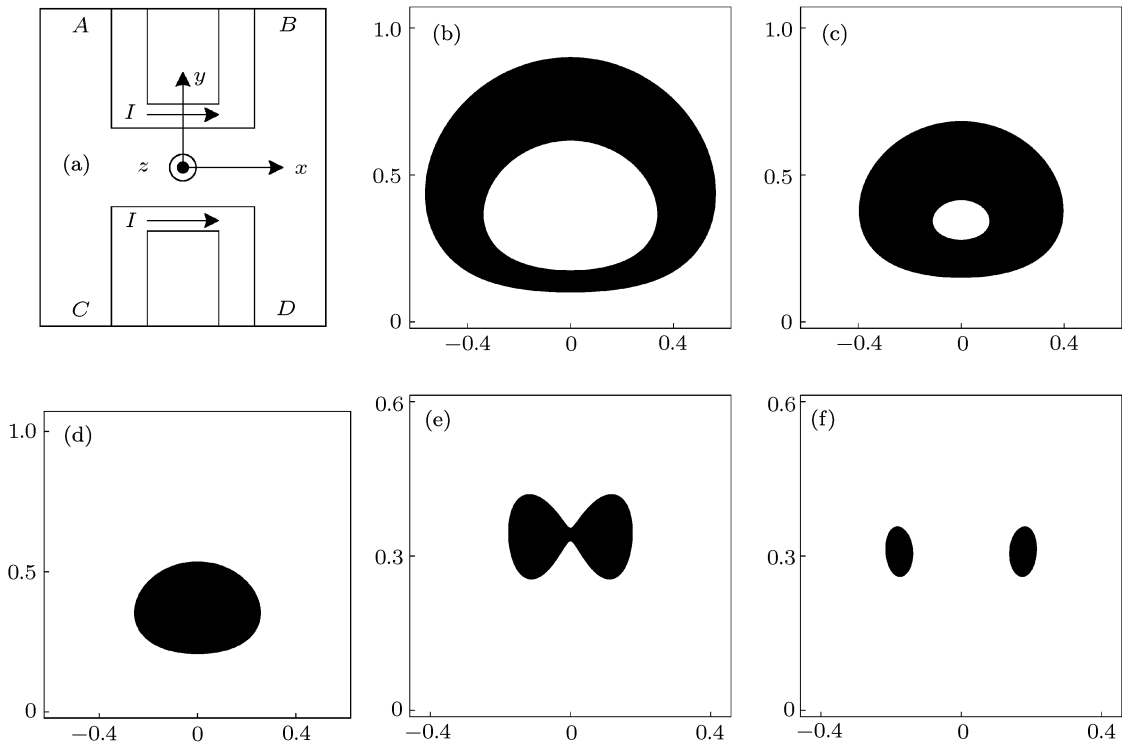


Fig.1. (a) Schematic diagram of the atom chip. A magnetic double well potential was created by superposing the magnetic field of two U-wires with current I and an external magnetic field B. The width of a U-wire is 200 μm, the distance between the central parts of the U-wires is 880 μm. The plots in Figs.5(b) to 5(d) show the equipotential lines with $\mu_B \times 0.8\times10^{-4}$ T in the xz plane for an increasing bias field B_y which is 5×10^{-4} T, 6.5×10^{-4} T, 7.7×10^{-4} T, respectively. Figures 5(e) and 5(f) are the equipotential lines in the yz plane for B_y which is 7.8×10^{-4} T and 1.0×10^{-3} T.

If a small magnetic field B_z in the z direction is applied during the splitting, the trajectories of the minima of the potential are completely different from the trajectories described above. For example, when $B_y < B_c$, a positive bias field B_z would divide the 'ring'-like trap into two separate quadruple traps and

make the higher one move to the left and the lower one to the right. A larger B_z makes the traps deviate more. Furthermore, the double wells do not merge completely at any B_y. When $B_y > B_c$, the symmetry of splitting can be broken as the two wells have opposite responses to B_z. A positive B_z makes the left well move upwards and the right downwards. Figure 2(a) shows the trajectories of the minima of the potential during the splitting with nonzero B_z. For negative B_z the responses of the traps are exactly opposite to those with positive B_z.

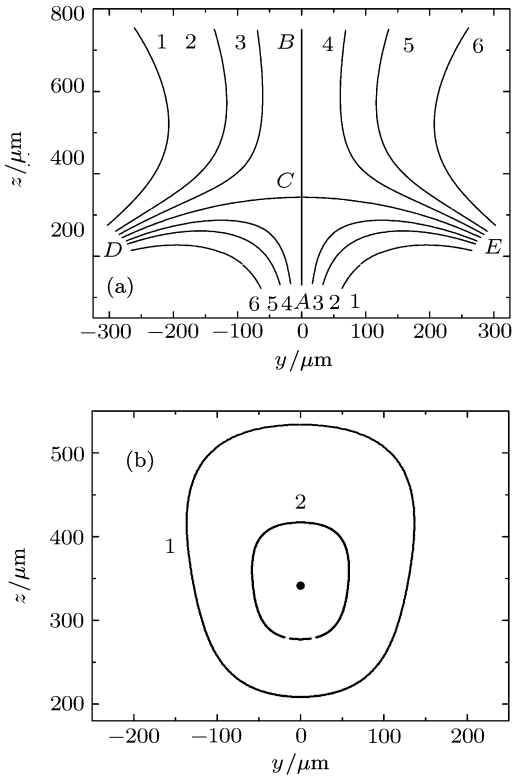


Fig.2. Splitting trajectories with a bias field with different directions and magnitudes. (a) When a critical bias field B_y=7.7×10^{-4} T is applied, a single hexapole trap is formed at the point C. As the field B_y is raised, the single trap would split symmetrically into two quadruple trap along the curve DE. If a small bias field B_z in the z direction is applied simultaneously during the splitting, the trajectories are not symmetrical and two minima do not merge at point C any more. The line AB is the perpendicular bisector. The trajectories 1, 2, 3, 4, 5, 6 are plotted for the bias field B_z which is 2×10^{-4} T, 1×10^{-4} T , 0.5×10^{-4} T, −0.5×10^{-4} T, −1×10^{-4} T, −2×10^{-4} T, respectively. (b) If a bias field $\boldsymbol{B} = B_c y + b(y\cos(\omega t) + z\sin(\omega t))$ is applied, the minima of the double well can be rotated on a ring around the merging point. The rings 1 and 2 are the trajectories of the minima of the double well for two different values of $b = 1 \times 10^{-4}$ T, 0.2×10^{-4} T, respectively.

Next, a special condition is considered. Starting from a single hexapole trap, we apply another rotating bias field $b = b(y\cos(\omega t) + z\sin(\omega t))$, where ω is the rotating frequency, and the magnitude of the rotating bias field $b \ll B_c$. At a certain moment t, the single trap will split into double wells whose minima are separated by a distance $d\sqrt{2b/B_c}$ and located on a line making an angle $\omega t/2$ with the y axis. For example, when a bias field $b = bz$ is applied, a double well tilted –45 degree will be created. When the bias field b rotates, the double well will rotate around the merging point at half the frequency.[9,18] The trajectories of double wells for different magnitudes of b are plotted in Fig.2(b).

Experimentally, we first transfer about 2×10^6 ^{87}Rb atoms prepared in the $5S$, $F = 2$, $m_F = 2$ state into a U trap whose minimum is located at (0, 200 μm, 380 μm), as described in Ref.[19]. The U trap is created by a current of 3 A sent through the U-wire CD and a bias field $B_y = 7.7 \times 10^{-4}$ T. Then a current through the U-wire AB increases from 0 A to 3 A in 200 ms; at the same time the current through the U-wire CD and the bias field B_y are kept constant. As a result, the atom cloud can be moved adiabatically to the position (0, 0, 340 μm) which is exactly the merging point of the double well potential and loaded into the single trap. Starting from the single trap, we can realize the symmetrical and asymmetrical splitting of atom cloud by varying the magnitude and direction of the bias field. In this work we use two probe beams to detect the splitting clouds, both of which are directed parallel to the surface of the chip. The one along the y direction is used to image the splitting along the perpendicular bisector, the other along the x direction is used to image the splitting in the y direction. In order to improve the image resolution, we use *in situ* imaging instead of time of flight (TOF) imaging. Due to the imperfection of the imaging beam near the chip surface, serious interference fringes are observed in the experimental pictures.

In the first experiment, we load the atom cloud into the single trap, and then vary the magnitude of the bias field B_y from the 7.7×10^{-4} T to different bias field magnitudes in 100 ms, at the same time ensuring that the bias field B_z is not present. When $B_y < 7.7 \times 10^{-4}$ T, a crescent-like, not the expected 'ring'-like, atom cloud is observed. Because of the high gradient of the lower part of the 'ring'-like trap, atoms have a very small probability of being loaded into the lower trap. Thus nearly all the atoms are loaded into the upper trap, resulting in a crescent-

like atom cloud. The distance between the crescent-like atom cloud and the merging point increases with decreasing B_y. When $B_y > 7.7 \times 10^{-4}$ T, dynamic splitting and recombination of the atom cloud are observed. Adiabatically increasing B_y from 7.7×10^{-4} T, the atom cloud initially at the merging point splits gradually into two separate atom clouds. The results of this experiment are displayed in Fig.3. Splitting is completely symmetrical and the distance between two atom clouds increases with increasing B_y. Figure 3(b) shows the trajectories of two separate atom clouds in the yz plane when the bias field B_y is varied. For the recombination of the two clouds, the process is reversed. A lot of experiments confirm that the symmetrical splitting and recombination are reproducible, which is crucial for the realization of atom interferometry. There is nearly no loss of atoms in the process of splitting and recombination.

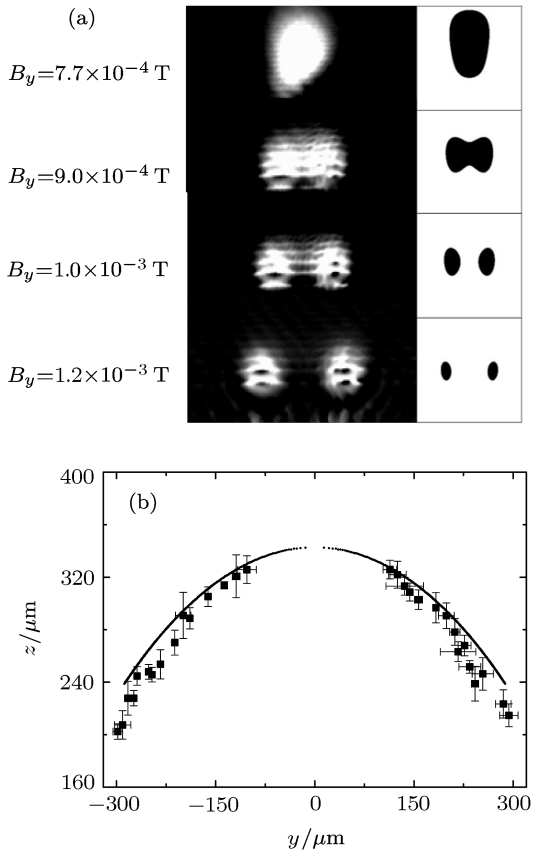
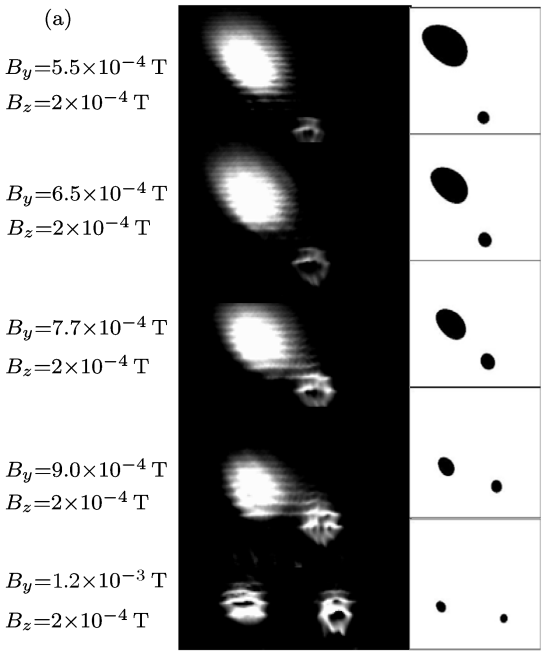


Fig.3. Symmetrical splitting of an atom cloud. A single trap is gradually split into a double well potential by ramping the bias field B_y from 7.7×10^{-4} T to 1.4×10^{-3} T. Absorption images (a) and trajectories (b) in the yz plane of the atoms during different splitting stages. The right column in (a) is the evolution of the equipotential lines which corresponds to a potential energy of $\mu_{\rm B}\times1\times10^{-4}$ T during the splitting process. The thick curve in (b) is the theoretical trajectories where the finite width of the U-wire is not considered.

In the second experiment we observe asymmetrical splitting of the atom cloud. Again, the experiment is initiated by loading an atom cloud into the single trap. Unlike the process of symmetrical splitting described above, a small bias field $B_z = 2 \times 10^{-4}$ T along the z direction is applied while the bias field B_y is varied. The asymmetrical splitting of an atom cloud is illustrated in Fig.4. When B_y is kept constant at 7.7×10^{-4} T, a single atom cloud is split into two separate atom clouds. The link between the two separate atom clouds is tilted at an angle of about –45 degree with respect to the perpendicular bisector. The atom number of the upper left one is much larger than the lower right one, because the upper left one has a larger capture volume. When the bias field $B_y < 7.7 \times 10^{-4}$ T, with the decrease of B_y, the upper left one will move upwards and far away from the perpendicular bisector, at the same time, the lower right one will move downwards and close to the perpendicular bisector. Furthermore, the gradient of the lower right trap increases gradually, leading to a smaller capture volume. As a result the atom number $N_{\rm L}$ in the left atom cloud is nearly 6 times larger than the number $N_{\rm R}$ in the right, shown in Fig.4(c). When $B_y > 7.7 \times 10^{-4}$ T, with the increase of B_y, the upper left atom cloud moves left and downwards, the lower right one moves right and upwards. Finally the trajectories of the two separate atom clouds tend to that of symmetrical splitting with a large B_y. Similarly the ratio $N_{\rm L}/N_{\rm R}$ of the atom number of the two separate clouds tends to 1:1, as shown in Fig.4(c).



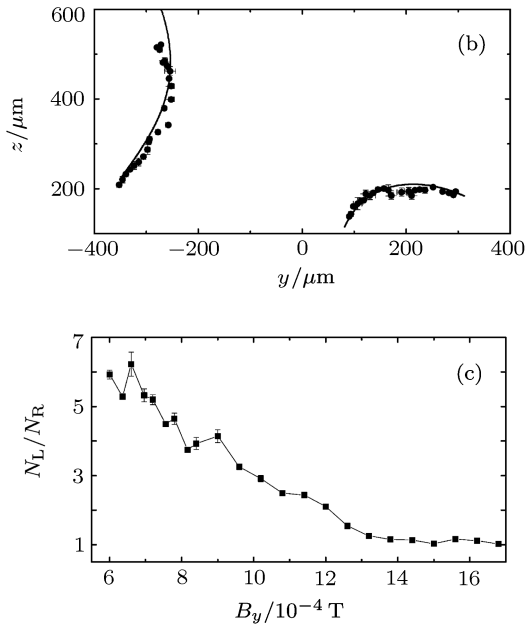


Fig.4. Asymmetrical splitting of an atom cloud. A single trap is gradually split into a double well potential by ramping the bias field B_y from 7.7×10^{-4} T to 1.4×10^{-3} T. Absorption images (a) and trajectories (b) in the yz plane of the atoms during different splitting stages. (c) The ratios N_L/N_R of the atom number in the left trap to that in the right trap vs the bias field B_y. With a large B_y, the ratio N_L/N_R tends to 1 : 1. The right column in (a) is the evolution of the equipotential lines which correspond to a potential energy of $\mu_B \times 1\times10^{-4}$ T in the yz plane during the splitting process. The thick curve in (b) is the theoretical trajectories where the finite width of the U-wire is not considered.

The realization of an atom interferometer needs not only to split an atomic wave packet coherently, but also to read out the relative phase between the splitting wave packets by recombination. Our experimental results show that two separate atom clouds do not recombine at any B_y, even if a much smaller B_z is presented. Therefore, one must eliminate the bias field B_z carefully during the symmetrical splitting and recombination of the atom cloud.

To further investigate the effect of the bias field B_z on the splitting process, we start from the single trap again, and apply a bias field B_z only, then observe the splitting process of an atom cloud. The experimental results are shown in Fig.5. The splitting is also asymmetrical: one atom cloud moves to the left upper side, the other one moves to the lower right side. The left upper atom cloud has a larger volume and thus more atoms. As the bias field B_z is increased, the trajectories of the left upper atom cloud deviate more from the line tilted by –45 degree and the lower right atom cloud moves closer and closer to the chip surface. When $B_z > 4\times10^{-4}$ T, the distance between the left upper atom cloud and the chip surface is nearly constant. When the bias field B_z returns to zero, two separate atom clouds merge into one atom cloud again. This asymmetrical splitting and merging can also be used in atom interferometers, especially in detecting the surface effect. During the splitting of the single trap, if a magnetic gradient is applied, a phase difference will be introduced between the two separate atom clouds due to their different distances from the chip surface.

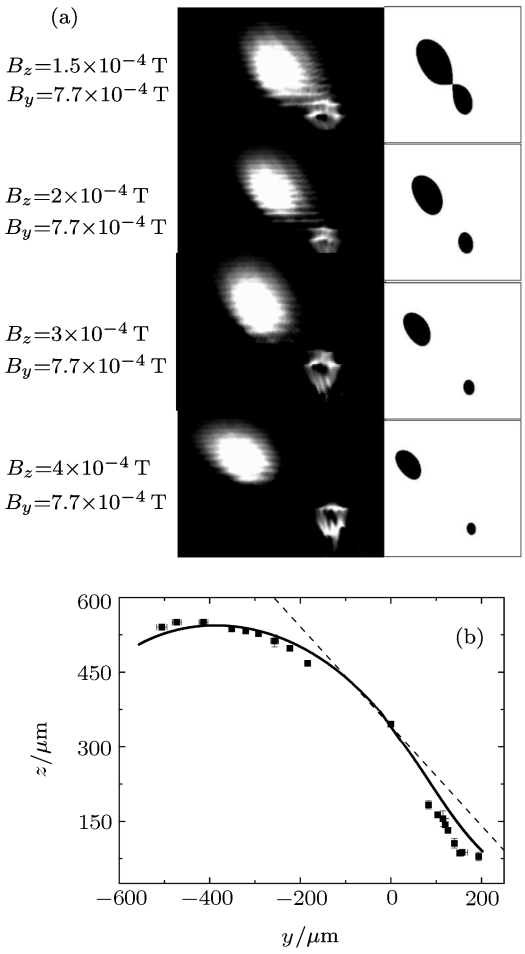


Fig.5. Splitting of an atom cloud with a varying bias field B_z and a constant bias field $B_y = 7.7\times10^{-4}$ T. The right column in Fig.5(a) is the evolution of the equipotential lines which correspond to a potential energy of $\mu_B \times 1\times10^{-4}$ T during the splitting process. The thick curve in Fig.5(b) is the theoretical trajectories where the finite width of the U-wire is not considered. The dashed line in Fig.5(b) is a line tilted by –45 degree.

However, one should keep in mind that the potentials produced by two U-wires are quadruple. The zero point in the quadruple trap limits the applications of the two U-wire scheme, such as splitting of Bose–Einstein condensation and atom interferometers. One

solution is to redesign a dual-layer chip like the design in Ref.[13], where two parallel wires on the upper layer are used for creating a double well potential and two perpendicular wires on the lower layer are used for providing the axial confinement and a nonzero bias field which can suppress Majorana spin flips.

In conclusion, we have demonstrated the dynamic splitting and merging of an atom cloud on an atom chip. The dynamic splitting is realized by deforming a single trap into a double well with two U-wires on an atom chip. Increasing the bias field in the y direction from the critical magnitude 7.7×10^{-4} T, we can realize symmetrical splitting in the horizontal direction at an arbitrary distance. If the process is reversed, two separate atom clouds will recombine in the merging point. If a bias field in the z direction is present during the splitting process, the symmetry of splitting will be destroyed, and at any B_y, the two separate atom clouds do not recombine. This asymmetry can be controlled by varying the directions and magnitudes of the applied bias field. Furthermore, we have investigated the trajectories of symmetrical and asymmetrical splitting in the yz plane, and they are consistent with the theoretical calculations.

Acknowledgement

We thank Tang J Y (Department of Physics, Zhejiang University) for fabricating the chip and Zhou S Y for some useful discussions.

References

[1] Fortágh J and Zimmermann C 2007 *Rev. Mod. Phys.* **79** 235
[2] Ott H, Fortágh J, Schlotterbeck G, Grossmann A and Zimmermann C 2001 *Phys. Rev. Lett.* **87** 230401
[3] Hänsel W, Hommelhoff P, Hänsch W and Reichel J 2001 *Nature* **413** 498
[4] Berman P R 1997 *Atom Interferometry* (San Diego: Academic Press)
[5] Kasevich M 2002 *Science* **298** 1363
[6] Wang Y J, Anderson D Z, Bright V M, Cornell E A, Diot Q, Kishimoto T, Prentiss M, Saravanan R A, Segal S R and Wu S J 2005 *Phys. Rev. Lett.* **94** 090405
[7] Günther A, Kraft S, Kemmler M, Koelle D, Kleiner R, Zimmermann C and Fortágh J 2005 *Phys. Rev. Lett.* **95** 170405
[8] Günther A, Kraft S, Zimmermann C and Fortágh J 2007 *Phys. Rev. Lett.* **98** 140403
[9] Hinds E A, Vale C J and Boshier M G 2001 *Phys. Rev. Lett.* **86** 1462
[10] Hänsel W, Reichel J, Hommelhoff P and Hänsch W 2001 *Phys. Rev.* A **64** 063607
[11] Andersson E, Calarco T, Folman R, Andersson M, Hessmo B and Schmiedmayer J 2002 *Phys. Rev. Lett.* **88** 100401
[12] Shin Y, Saba M, Pasquini T A, Ketterle W, Pritchard D E and Leanhardt A E 2004 *Phys. Rev. Lett.* **92** 050405
[13] Shin Y, Sanner C, Jo G B, Pasquini T A, Saba M, Ketterle W, Pritchard D E, Vengalattore M and Prentiss M 2005 *Phys. Rev.* A **72** 021604(R)
[14] Schumm T, Hofferberth S, Andersson L M, Wildermuth S, Groth S, Bar-Joseph I, Schmiedmayer J and Krüger P 2005 *Nature Physics* **1** 57
[15] Jo G B, Choi J B, Christensen C A, Lee Y R, Pasquini T A, Ketterle W and Pritchard D E 2007 *Phys. Rev. Lett.* **99** 240406
[16] Brugger K, Krüger P, Luo X, Wildermuth S, Gimpel H, Klein M W, Groth S, Folman R, Bar-Joseph I and Schmiedmayer J 2005 *Phys. Rev.* A **72** 023607
[17] Cassettari D 2000 *Cold Aloms in Microscopic Traps: from Wires to Chips* Ph.D thesis University of Innsbruck, Austria
[18] Estéve J, Schumm T, Trebbia J B, Bouchoule I, Aspect A and Westbrook C I 2005 physics/0503112
[19] Ke M, Yan B, Li X L and Wang Y Z 2008 *Chin. Phys. Lett.* **25** 907